

A Ripple Voltage Sensing MPPT Circuit for Ultra-Low Power Microsystems

Inhee Lee, Suyoung Bang, Dongmin Yoon, Myungjoon Choi, Seokhyeon Jeong, Dennis Sylvester, David Blaauw
University of Michigan, Ann Arbor, MI

Abstract

We propose a maximum power point tracking (MPPT) circuit for micro-scale sensor systems that measures ripple voltages in a switched capacitor energy harvester. Compared to conventional current mirror type MPPT circuits, this design incurs no voltage drop and does not require high bandwidth amplifiers. Using correlated double sampling, high accuracy is achieved with a power overhead of 5%, even at low harvested currents of 1.4 μ A based on measured results in 180nm CMOS.

Introduction

A number of miniature sensor nodes were recently proposed for use in new embedded application areas, including medical, security, and resource exploration. In general, miniature-scale systems are equipped with a harvesting unit (solar, thermal, etc) to recharge their battery. The small form factor of these sensors has led designers to opt for integrated switched capacitor boost converters (SCBCs) with a total capacitance in the range of 0.5 to 1.5nF [1,2]. Furthermore, the limited size of the harvesting unit makes efficient energy extraction from the energy source and up-conversion of the voltage a majority priority. However, the type of energy source and its operating point can vary greatly. For instance, in office lighting a 1mm² solar cell reaches its optimal energy efficiency at ~250mV and produces 45nA current. In sunlight, that same solar cell has optimal energy efficiency at ~350mV and produces 2 μ A. Clearly, the two conditions require vastly different capacitor switching frequencies, switch sizes, and voltage conversion ratios of the SCBC. A highly flexible SCBC is therefore needed that ideally performs maximum power point tracking (MPPT), allowing it to automatically search for and track the configuration that delivers maximum power to the battery.

In general, MPPT involves simultaneous measurement of both voltage and current delivered to the battery, which are multiplied and fed into a search algorithm. Given the small power budget of micro-sensors, the voltage/current measurement and search algorithm must be performed with minimum power overhead. A comprehensive MPPT method was proposed in [3] where the battery inflow current is measured (Fig. 1). While having the advantage of directly measuring energy delivered to the battery, it incurs a voltage drop over the current mirror transistor, resulting in significant energy loss. Furthermore, it requires a high bandwidth amplifier to track dynamic current influx.

This paper demonstrates a MPPT circuit that takes advantage of the unique structure of SCBC – it places a small sampling capacitor in parallel with the flying or decoupling cap in the SCBC that “eavesdrops” on the voltage transfer that occurs in the voltage converter. By integrating the small voltage fluctuations using correlated double sampling (CDS), the power delivered to the battery can be determined. Since the sampling capacitor is 64.8 \times smaller in size than the flying cap, the impact on conversion efficiency is negligible. By directly tracking power delivered to the battery all parameters of the SCBC can be optimized, including switching frequency, switch size, and conversion ratio.

Proposed Circuit

Fig. 2 shows the circuit diagram of the proposed harvested energy monitor and its waveform. The SCBC has a ladder topology and its switches are driven by a set of non-overlapping clocks (Φ_1 and Φ_2). This switching function transfers charge from the energy source to the battery, generating ripple voltages at SCBC internal nodes. In one phase (Φ_1), the flying capacitor of C_{FLY2} provides charge to the decoupling capacitor of C_{DC1} by charge sharing while the flying capacitor of C_{FLY1} transfers charge to and recharges the battery. Thus, voltage across C_{DC1} (V_{DC}) increases while voltage across C_{FLY1} (V_{FLY}) decreases when energy is harvested. In the other phase (Φ_2), charge moves from C_{DC1} to C_{FLY1} due to $V_{DC} > V_{FLY}$ and V_{DC} decreases while V_{FLY} increases (Fig 2 waveforms). This voltages difference ($V_{DC} - V_{FLY}$) is proportional to the amount of charge sent to the battery in a switching period. Hence, integrating the ripple voltages’ difference for a fixed time provides a measure of harvested energy.

We implement the proposed ripple voltage sensing circuit using a small sampling capacitor (C_{SAMPLE}) that is placed in parallel with C_{FLY1} , a correlated double sampling integrator, two integration capacitors (C_{INT1} and C_{INT2}), and a clocked comparator. To sample V_{DC} and V_{FLY} , C_{SAMPLE}

is alternatively connected in parallel to C_{DC1} or C_{FLY1} . Its sampling frequency is divided down to ~1kHz from Φ_1 to relieve the bandwidth requirement of the integrator and hence its power consumption. The small size of C_{SAMPLE} , along with the fact it is decoupled from the SCBC only once in 138 cycles, results in negligible energy impact on SCBC (<0.91% efficiency degradation, measurement-based calculation including phase drivers).

One challenge in measuring energy transfer in the proposed method is the small magnitude of the ripple, which is a requirement in high efficiency voltage conversion. As a result, the integrator’s output voltage can easily saturate due to accumulation of the amplifier’s offset or low frequency noise over multiple integration cycles. To address this, we use CDS to integrate the differences of V_{FLY} and V_{DC} ripple and amplify it sufficiently for use in the comparator. CDS is achieved by changing the polarity of C_{INT1} and C_{INT2} with P_1 and P_2 . The energy transfer is calculated for two configurations successively and stored on C_{INT1} and C_{INT2} . These two capacitor voltages are then compared (READ and FIRE) to determine the optimal energy transfer configuration and the SCBC parameters are updated accordingly.

The complete energy harvesting unit consists of a reconfigurable SCBC, harvested energy monitor, MPPT controller, look-up table, and a wide frequency range oscillator (Fig. 3). The MPPT controller can adjust four SCBC parameters through the look-up table: conversion ratio, switching frequency, switch size, and gate driving voltage. Mapping of switching frequency, switch size, and gate driving voltage is done in the programmable look-up table. This allows inefficient or non-functional parameter combinations to be excluded from the search. The look-up table also sends the clock division ratio (HEMCLK_DIV) to the harvested energy monitor to set the integrator frequency.

The designed SCBC connects a successive approximation (SA) DC-DC converter [4] in series with a 1:6 converter (Fig. 4). Each switch has transistor size controllability (1 to 63) to optimize switching loss and conduction loss for different switching frequencies. The smallest switches have separate smaller flying capacitors while larger switches share larger ones since the SCBC does not require large switches for slow switching frequency, while capacitance from large switches deteriorate its efficiency [5]. AC coupling gate drivers enable the modulation of gate driving voltage by only changing the amplitude of Φ_1 and Φ_2 . They level shift Φ_1 and Φ_2 to the proper voltages based on switch source voltages, which is stabilized by decoupling capacitors. Compared to the conventional AC coupling gate drivers for the SA converter, new gate drivers are proposed for the 1:6 converter because of its single-phase topology and the fixed 0.6V between V_{HIGH} and V_{LOW} . This design requires only half the capacitors by reusing signals from the complementary type of gate driver in order to short gate and source of switch transistors to prevent DC drift. Also, devices connected to V_{HIGHER} and V_{LOWER} help reduce leakage via super cut-off when the switches are disabled.

Measurements

Fig. 5 shows that the fine resolution of conversion ratio enables > 94.6% tracking efficiency across 170 – 4100 incident lux despite inherent limitations of SCBCs compared to inductive boost converters. The designed MPPT circuit consumes 35nW (avg. over light intensity) and achieves a power overhead of 5%, even at low harvested currents of 1.4 μ A (Fig. 6). Fig. 7 shows example MPPT operation including changing conversion ratios and switch sizes. From the last position, the MPPT searches for the updated maximum power point (MPP). The MPPT locks converter configuration once finding MPP while it checks other configuration periodically for improved energy harvesting. A comparison to recent work is given in Table 1, showing > 6 \times improvement in terms of MPPT circuit power. Die photo is given in Fig. 8.

References

- [1] Y. Shih *et al.*, TCAS2, 2011.
- [2] G. Chen *et al.*, ISSCC, 2011.
- [3] I. Doms *et al.*, JSSC, 2009.
- [4] S. Bang *et al.*, ISSCC, 2013.
- [5] Y. Ramadass *et al.*, JSSC, 2010.
- [6] S. Bandyopadhyay *et al.*, VLSI, 2011.
- [7] Y. Qiu, *et al.*, ISSCC, 2011.
- [8] C. Huang *et al.*, ESSCIRC, 2012.

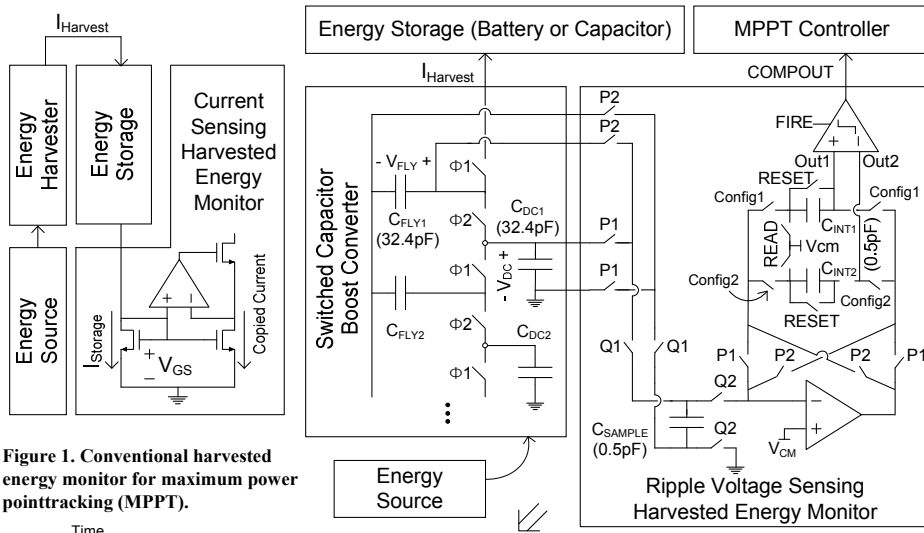


Figure 1. Conventional harvested energy monitor for maximum power tracking (MPPT).

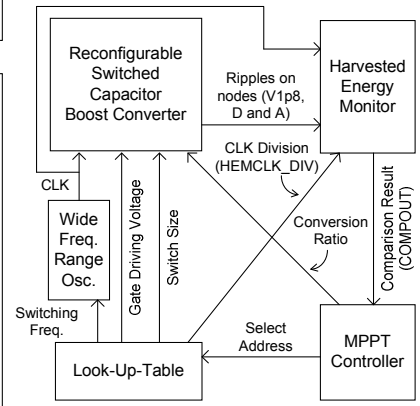


Figure 3. Block diagram of the designed energy harvesting unit.

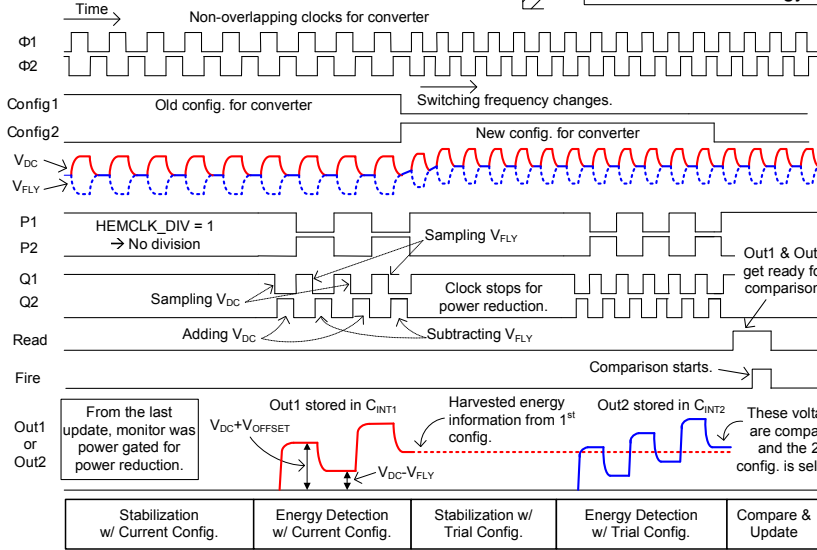


Figure 2. Proposed ripple voltage sensing harvested energy monitor and its waveform.

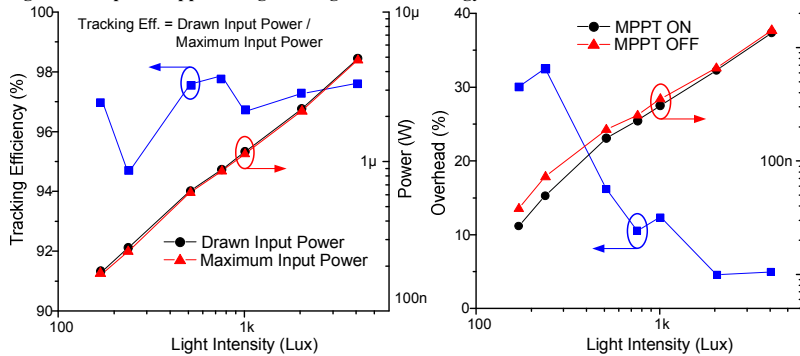


Figure 5. Tracking efficiency over light intensity.

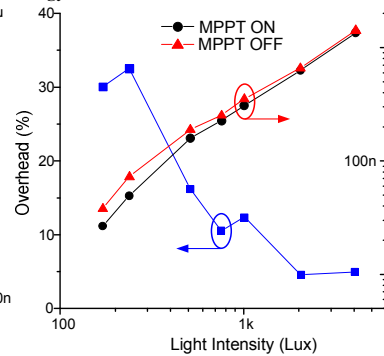


Figure 6. MPPT overhead over light intensity.

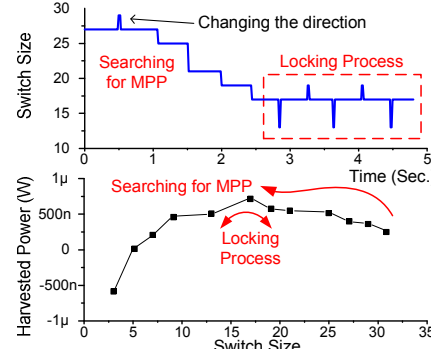
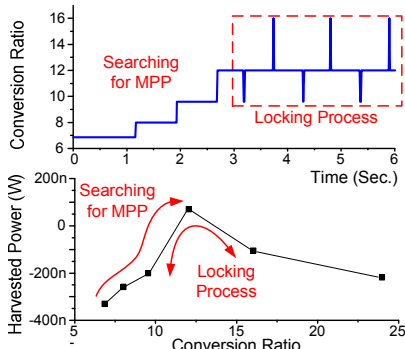


Figure 7. Examples of MPPT operation with conversion ratio (left) & switch size update (right): Configuration update in time domain (top) & Improved harvested power by configuration update (bottom).

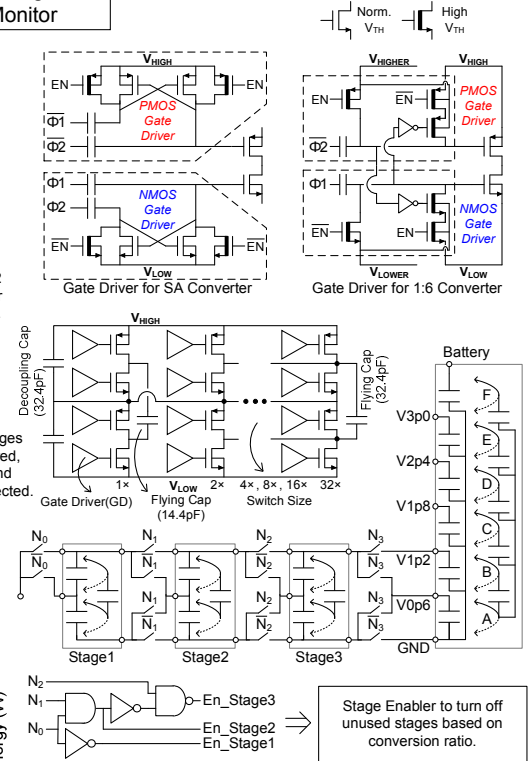


Figure 4. Reconfigurable switched capacitor boost converter.

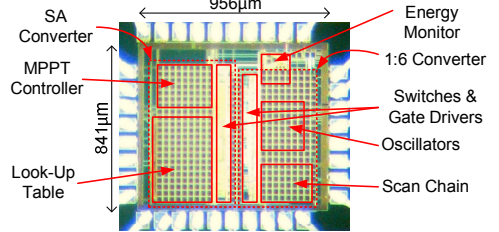


Figure 8. Die photo.

Parameter	This Work	[3] JSSC 2009	[6] VLSI 2011	[7] ISSCC 2011	[8] ESSCIRC 2012
Process	180nm	350nm	350nm	250nm	180nm
Boost Converter Type	Capacitive	Capacitive	Inductive	Inductive	Inductive
Tracking Efficiency	94.6%	N/A	95.0%	80.5%	99.6%
MPPT Circuit Power	35nW	2μW	6μW	2μW	234nW
MPPT Method	Hill-Climbing	Hill-Climbing	Hill-Climbing	Analog	Mixed-Signal

Table 1. Performance summary and comparison.